Deep Learning Assisted Plus Disease Screening of Retinal Image of Infants

Vijay Kumar[1], Vatsal Agrawal[2], Shorya Azad[3] and Kolin Paul[1,2]

[1]*Khosla School of Information Technology, Indian Institute of Technology, Delhi, India*
[2]*Department of Computer Science and Engineering, Indian Institute of Technology, Delhi, India*

[3]

Keywords: Fundus Image, Retinopathy of Prematurity (ROP), Plus Disease, Generative Adversarial Network (GAN), U-Net, Blood Vessels Segmentation, Deep Learning (DL), Vessel Tortuosity.

Abstract: Retinopathy of Prematurity (ROP) is the leading cause of blindness in premature infants in developing countries. The international classification of ROP (ICROP) classifies ROP based on location, severity, and stage. Plus disease is a crucial feature in ROP classification. Plus is the most severe form of vascular dilatation and tortuosity, and it causes severe ROP and visual loss if untreated. Despite decades of research, identifying and quantifying Plus diseases is challenging. Understanding and detecting Plus in ROP patients can help ophthalmologists provide better treatment, restoring vision to many infants with severe ROP. Hence, we have proposed a robust Deep Learning-assisted framework for Blood Vessels map generation and analysis that may effectively address the issue related to Plus disease screening and monitoring. We have extensively studied various methods for computing and locating different blood vessel map features such as vessel branch point, vessel width, vessel skeleton/centre-line, vessel segment tortuosity, etc. Additionally, we divided the branches into two levels based on the width of the branches. For our investigations, we have used both local and public databases. This work also includes a detailed analysis of these datasets' vascular feature and their level.

To the best of our knowledge, none of the publicly available models could independently classify branches and/or analyse the tortuousness based on the parent and child relationship of branches. For Plus, pre-Plus, and Healthy infants, the average tortuosity index is 1.959, 1.1530, and 1.126, and the percentage of vessels severely infected is 44%, 30%, and 20%, respectively. Moreover, our algorithm recognises and analyses many vessels. The precision of many parameters is remarkable.

1 INTRODUCTION

Retinopathy of prematurity (ROP) is one of the most common causes of retinal disease in preterm newborns across the world (Organization et al., 2019).

The International Classification of ROP (ICROP) classifies ROP into three zones, and five stages based on its anteroposterior position (area), severity (stage), and vascular features (disease severity) (Chiang et al., 2021). Plus disease is another condition in which the central and posterior retinal blood vessels become dilated and tortuous, as shown in Figure 1. In the ROP disease classification system, Plus disease is a key factor (Chiang et al., 2021). Plus disease causes permanent vision loss if left untreated. Additionally, the neonatal care division and ophthalmologists have limited time to provide appropriate care, and prognosis for these patients, which further worsens the condition and leads newborns to be at risk of ROP-induced
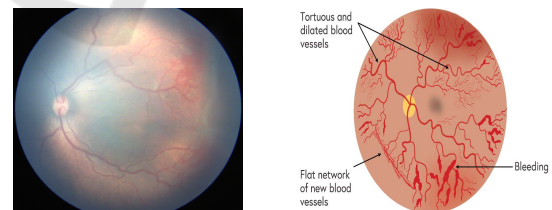
(a) ROP Zone-2 with Plus.   (b) Plus disease symptoms.

Figure 1: Example infant's retinal images with ROP-plus disease.

visual impairment (Tian et al., 2019).

Classification of Plus disease is mostly based on the tortuosity and dilatation of blood vessels (Tian et al., 2019). Tortuosity refers to the curvature of arteries and veins. Despite decades of scientific research, it remains difficult to identify and quantify vascular abnormalities (i.e., tortuosity and dilation) accurately for Plus disease (Tian et al., 2019). Under-

standing vascular phenomena in ROP patients could lead to the development of alternative treatment options that could restore the vision of a substantial number of severely affected ROP patients. Therefore, vessel analysis may be an effective strategy for addressing this problem.

Given its importance, authors have developed several Plus disease diagnostic and classification algorithms using image processing, computer vision, and machine learning (ML) or deep learning (DL). In the last few years, ML/DL algorithms have significantly improved the performance of Plus disease diagnostic and classification algorithms (Reid and Eaton, 2019; Tian et al., 2019). Although DL-based methods can accurately detect and classify Plus, they do not provide a comprehensive and quantitative understanding of the disease. As a result, ophthalmologists often cannot link the results of the DL-based approach to clinical symptoms. Furthermore, DL-based systems are data-driven and require a large amount of labeled pathological data for training, testing, and validation. In the case of ROP disease, acquiring many fundus images of infants is difficult due to the lack of publicly available datasets on the disease (Scruggs et al., 2020). As a result, the advancement and usage of DL-based methods in clinical use are restricted (Razzak et al., 2018).

Therefore, this paper presents a solution for providing interpretable results, which can be used in clinical settings by utilising a DL-assisted system that can clearly detect and classify Plus disease by analysing the blood vessels' tortuosity.

The remainder of the paper is organized as follows. Section 2 highlights related studies on ROP-Plus disease screening and monitoring. Section 3 describes the proposed DL-assisted approach for ROP-Plus disease screening in detail. Section 4 provides results of various pipeline stages of the proposed technique. Finally, Section 5 concludes the papers and discusses how the work can be extended in the future.

2 RELATED WORK

Over the years, ophthalmologists have adopted many ROP-Plus screening and diagnostic procedures. In manual screening, an ophthalmologist uses a retinal image to examine the signs of ROP disease. This is an inefficient and biased method (Reid and Eaton, 2019; Ting et al., 2019). As a result, objective evaluation is important. Several approaches assist the physician and ophthalmologist with computer-assistive diagnosis (CAD) using various disease screening tools (Doi, 2007). For instance, (Oloumi et al., 2016) ex-

plored CAD to establish some conventional ways to aid physicians in making objective detection. In addition, the fact that standard methods (based on image processing and computer vision) can only extract basic information from fundus pictures, which is insufficient to increase the accuracy of neonatal retinal image classification (Razzak et al., 2018). When light is uneven, the contrast between the lesion and the surrounding typical region is negligible, making fundus images challenging to interpret and lesion characteristics to be obscured (Kumar. et al., 2022). Therefore, an ML and particularly DL-based technique is required to extract in-depth, high-level information that enables automated ROP-Plus screening.

The self-learning capability of DL and its efficiency and accuracy have attracted researchers' interest (Scruggs et al., 2020; Ting et al., 2019). Its applications in ophthalmology have proven successful, particularly in detecting image features of the retina associated with glaucoma, age-related macular degeneration (AMD), diabetic retinopathy (DR), cataract, and ROP (Ting et al., 2019). These are data-driven approaches in which the DL model is pre-trained on similar pathological datasets associated with the disease. DL-based solutions surpass traditional CAD applications in terms of performance. The DL-based screening method overcomes the rule-based system's flexibility and adaptability constraints (Razzak et al., 2018).

For training, testing, and validation, DL-based systems require a large amount of labelled and unlabelled data (Ting et al., 2019; Razzak et al., 2018). Data collection (pathological, medication, and treatment history) and labelling are time-consuming procedures for medical applications (Razzak et al., 2018; Ting et al., 2019). In some contexts, a disease's occurrence is restricted, and its features are influenced by socioeconomic factors and regional boundaries, making it challenging to obtain high-quality critical information. In (Ting et al., 2019), the authors introduced DCNN-based reinforcement learning methods for ROP that alleviate the developer's/researcher's additional burden of labelling the DL model prior to training. Whereas the trained deep learning model is fast and effective on a particular dataset, its performance on any other dataset is uncertain. Additionally, it is challenging for an expert to understand and describe the relationship between the clinical manifestations of the disease and the DL result (Scruggs et al., 2020).

Therefore, we presents a DL-assisted ROP screening technique to address these issues where large historical datasets are lacking and interpretation of DL-based system results is required.
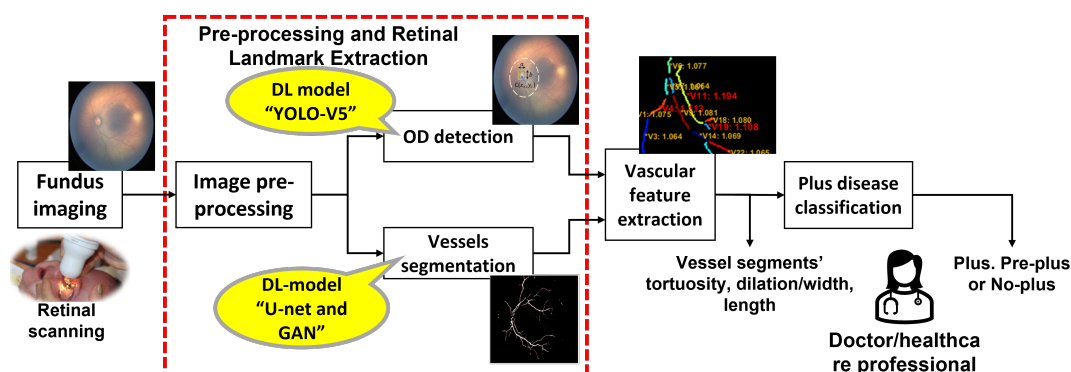
Figure 2: DL assisted fundus image feature extraction and Plus disease screening.

3 SYSTEM ARCHITECTURE

The detailed architecture of the proposed system is shown in Figure 2. It consists of four functional units:

- Fundus imaging (or retinal scanning) unit.
- Image pre-processing and retinal feature extraction .
- Post-processing and vascular feature extraction.
- Disease classification.

3.1 Neonatal Fundus Imaging and Data Preparation

The ophthalmologist or clinician acquired retinal images using the RetCam-3 fundus camera. RetCam-3's image resolution is 1600 x 1200 pixels. An infant's eye examination requires around ten photographs. Figure 3 shows images of the retinas of premature infants. Neonatal ophthalmologists use these images in the diagnosis and monitoring of ROP as well as other diseases. As, the quality of the picture is often inadequate (because of uneven lighting, blurry motion, wrong set-up device, etc.) it is difficult and time-consuming to detect and follow the pathological changes induced by newborns. Therefore, we used image reconstruction and enhancement methods

Table 1: Retinal image datasets used for training and testing of OD, blood vessel segmentation and Plus disease classification modules (Here, NA: not available).

Dataset Name	Number of images (in OD)	Number of images (in vessels segmentation)	Number of images (Plus)
ARIA	N/A	143	N/A
DRHAGIS	N/A	40	N/A
STARE	297	20	N/A
FIRE	224	N/A	N/A
DRIVE	40	20	N/A
HRF	45	45	N/A
IDRiD	511	N/A	N/A
AIIMS	439	6	395
Total	1556	274	395

Table 2: AIIMS Dataset with 3-class Plus classification.

no_Plus	pre_Plus	Plus	Total
73	109	213	395

to improve quality and reduce the noise of scanned images, discussed in Section 3.2.1.

In order to train, test, and validate the proposed system, especially the DL-based models, a large amount of historical data is required. Therefore, we created different sets of fundus datasets for training, testing, and validation of different modules as per the availability of relevant historical data points (or images).

As shown in Table 1, we labelled 1556 fundus pictures for the OD model. On the other hand, we used 274 images for training and testing the vessel segmentation module. In addition, to test the effectiveness of the segmentation model, we annotated the blood vessels in an image of a preterm infant's retina as ground truth. The process of vessel annotation is time-consuming and laborious. Hence, six blood vessels have been annotated in each image.

For the ROP disease, no fundus image datasets are available publicly. Hence, In order to build the ROP-Plus screening and classification system, we have use 439 images from the AIIMS dataset for ROP disease (Kumar et al., 2021; Kumar et al., 2022). Further, a neonatal ophthalmologist classified and labeled these images into three groups based on the severity of Plus disease: Plus, Pre-Plus and Normal. Table 2 summarizes the overall number of Plus, Pre-Plus and No-PLus preterm infants' retinal scan images in the AIIMS dataset.

We used datasets in two phases for the suggested system of this research. In the first phase, we used it for training and testing extraction models for retinal features (OD and blood vessel map), and in the second, we used it for training and testing to classify the image as Plus, Pre-Plus, and Healthy.
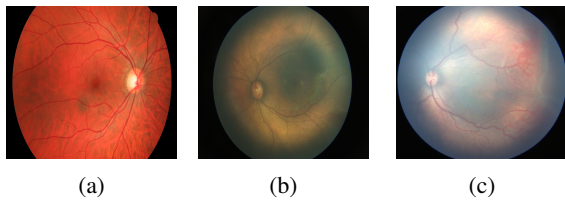
Figure 3: Example images from the retinal vessel segmentation and OD datasets. Left to right: (a) DRIVE: retinal image of elderly people that are publicly available; (b) AIIMS image: retinal images of newborns' healthy eyes with no-ROP and no-Plus disease; and (c) AIIMS image: retinal images of infants' unhealthy eye with +ve ROP Zone-2 and +ve Plus disease.

3.2 Image-Preprocessing and Retinal Feature Extraction

3.2.1 Image-Preprocessing

This section describes the image pre-processing methods used by the proposed system to reduce the amount of noise in retinal scans. The neonatal's fundus image is pale yellowish. We preferred the G-channel and used it in subsequent image-processing modules (Kumar et al., 2021; Kumar. et al., 2022; Kumar et al., 2022). We utilized a median, average filter, and contrast-limited adaptive histogram equalization (CLAHE) to enhance the quality of the colour image and eliminate illumination variations and blurriness (Kumar et al., 2021). However, the colour image is employed as an input in the DL system for feature extraction, disease diagnosis, and classification.

3.2.2 Retinal Feature Extraction

In this section, we discuss the DL-based image analysis methods used to extract retinal image feature's OD and blood vessels map.

OD Detection: The accuracy of a Plus classification is governed by the fact that how well the OD location is recognised (because the reference point required for the vessel tracing is started from the optical nerve boundary in retinal images) and how well the vessel segments are detected by tracing. For the OD detection, we have used (Kumar et al., 2021). In which, authors used pre-trained DL-models, YOLO-v5 (Jocher et al., 2021) for OD detection. Further, labelled the compiled dataset as per the YOLO model's input and then trained the network with a 416x416 input pixel resolution, summarised in Table 1.

Blood Vessels Segmentation: The retinal blood vessel map is the most significant retinal feature

used for tortuosity analysis in the proposed system. Blood vessels of the preterm infant retina are not distinguishable from the background as preterm infants' retinal blood vessel systems are not fully developed at the time of birth, as shown in Figure 3. Therefore, conventional vessel segmentation methods, which perform well with publicly available retinal image datasets, do not work well with an infant's retinal image. Hence, for vessels segmentation, a Pix2Pix-GAN (Isola et al., 2018) or U-Net (Ronneberger et al., 2015) architecture-based vessel segmentation method is used (Kumar. et al., 2022). Further, we have use same approach for training and testing as proposed in (Kumar. et al., 2022) and used publicly available image datasets listed in Table 1.

3.3 Vascular Feature Extraction

To understand and quantify the ROP-Plus disease progression and severity, vascular features analysis is required. This includes analysis of blood vessels' tortuosity which requires the vessel's skeleton, branch points, width, length, and blood vessels end points. For the vascular feature extraction, we have use image-processing and computer vision based method is shown in Figure 4. In this flow chart, it performs the following steps to compute blood vessel (BV) features (which includes BV segment curve length (S), chord length (D), and order of BV segments(O)):

1. Centreline finding
2. Noise removal followed by branchpoint and end point detection.
3. Branch points removal and BV segmentation.
4. Segment length (or curve length) and Segment chord calculation.
5. Tortuosity Calculation.
6. Ordering of blood vessels segments based on blood vessels width.

Centreline Finding. Centreline can be found with the help of a technique known as skeletonization. Skeletonization is morphological operation. Matlab support many skeletonization of a 2D binary image function includes "bwskel", "skel" and "thin". In general, it is found that erroneous branch points are discovered due to one-time skeletonization, as it is possible for a point that is not a branch point to have three pixels to be adjacent to each other in the condition of highly tortuous arteries. So, we have used 'thin' for the removal of short-end branches and spurs as it may also include unnecessary extra pixels in the curved region. We then used 'bwskel' for centreline due to its accuracy.
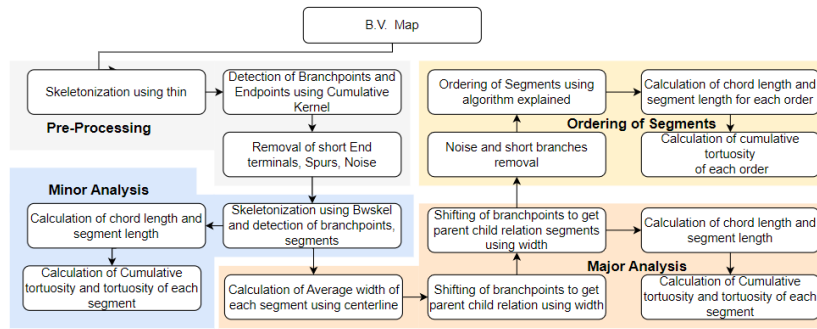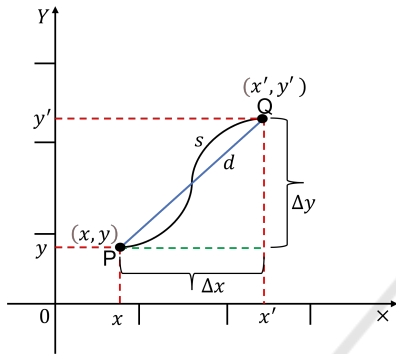
Figure 4: Blood vessels feature extraction.

Figure 5: Illustration of segment (*PQ*) is used to estimate blood vessel tortuosity by examining segment length (*s*) with respect to its chord length (*d*).

Branch Point and end Point Detection. In this stage, the branch-points and endpoints of the blood vessel network are identified. The tortuosity level must be measured, analyzed, and quantified by locating the branch-points of a skeletonized vascular network. Branch points are recognized via a morphological process that identifies them, dilates them, and reserves the branch point pixels that split various segments (Wang et al., 2021; Sukkaew et al., 2008). Therefore, we used Matlab's morphological operation to the binary image centerline with a simple kernel to detect branch points with an adjacency of central pixels greater than 2 (MathWorks, 2023). After segmentation, vessel segments are used for a tortuous assessment.

Segment Length and Chord Length Calculation. Vessel segment's attributes segment length (*S*) and chord length (*D*) are used for tortuosity calculation are define below:

- Segment length or Geodesic distance (*S*): The maximum non-infinity quasi-Euclidean distance between any two endpoints of the segment's centerline skeleton (*PQ* as shown in Figure 5) is used to determine the arc-length distance between the

start and endpoints of the segment, as follows:

$$S(\gamma(Q) - \gamma(P)) = v * |Q - P|, \quad (1)$$

where, $v \geq 0$.

- Straight line distance (Chord): It is the straight-line distance (Euclidean distance) between two ends (*PQ* as shown in Figure 5) of the skeleton's centerline segments, as follows (Heneghan et al., 2002):

$$Chord(D) = \sqrt{(x'-x)^2 + (y'-y)^2}, \quad (2)$$

where, (x,y) and (x',y') are the co-ordinate of segmented blood vessel's start and end point, *P* and *Q* respectively.

Tortuosity Calculation. For the tortuosity calculation, we have used two approaches. The first approach, proposed by (Hart et al., 1997), is the simplest and most widely used measure for calculating tortuosity. It computes the tortuosity of a vessel by examining how long the curve is relative to its chord length, as follows:

$$\text{Tortuosity}(\tau_H) = \frac{\text{Curve length}(S)}{\text{Chord length }(D)} - 1, \quad (3)$$

where *S* is the arc length or curve length obtained by counting all the points (or pixels) from the start of the vessel to its end, and *D* is the length of the underlying chord.

There was another kind of method described by (Grisan et al., 2008). This technique works by first segmenting each vessel into *n* segments of constant-sign curvature and then combining these segments and their respective numbers to compute as follows:

$$\text{Tortuosity}(\tau_G) = \frac{n-1}{S} \sum_{i=1}^{n} [\frac{s_i}{d_i} - 1], \quad (4)$$

where *S* is the vessel arc length, s_i is the subsegment arc length, and d_i is the subsegment chord length.

Ordering of Segmented Branches. Further, for the analysis of retinal vascular structure, we have used two types of blood vessel (BV) segmentation and labelling methods: (1) the minor analysis model and (2) the major analysis model. In the minor analysis model, we simply break vessels at branch points. In the major analysis model, we break vessels at branch points while maintaining parent-child relations.

The first is only to increment the number if its value is smaller than the others. This approach is appropriate for two to three-level categorization. The second method involves increasing the number without limits. This method is sometimes better for images with more than three levels, but the level threshold must be set manually for each new image. Repeat the above step at least four more times to get the final output, which can be further used by the tortuosity calculation algorithm to get a detailed analysis of vessels. A two-level system is good enough for images with a lot of noise, and a three-level system is good enough for regular fundus image. However, higher-level systems sometimes suffer from a false loop issue.

3.4 Disease Classification

Disease classification is the fourth and final functional unit. In the proposed system, we classified the severity of PLUS disease using two rule-based approaches.

Percentage of Infected Vessels: Computes the proportion of vessel segments whose curvature index exceeds the threshold curvature index (T_H). Here, T_H is the mean tortuosity index of the vessel segments in the healthy fundus image.

Cumulative Curvature Index: It estimates the curvature index of vessel segments using equation (4), treating all fundus image segments as sub-segments of a segment.

After that, we utilized the ROP-Plus dataset to compute these threshold values for Plus disease classification (i.e., healthy, pre-Plus, and Plus) using both of the above mentioned approaches. Using a training dataset (listed in Table 2), all threshold values were computed. The remaining dataset is utilized to test the suggested system.

4 RESULTS AND DISCUSSION

The proposed system and its different modules are implemented and tested on a workstation with Intel(R)

Xeon(R) 40-Core CPU E5-2630 v4 @ 2.20GHz with 64 GB RAM and 8 GB NVIDIA GeForce GTX 1070 GPU. Further, we used online Matlab to post-process the segmented blood vessel map. In this section, we discuss the results of the proposed method for vascular feature analysis to detect and classify infant ROP-Plus.

4.1 Retinal Feature Extraction

We have used YOLO-v5 and Pix2Pix-GAN Or UNet models to extract retinal characteristics (i.e., OD and retinal blood vessel nap). Both algorithms have also shown excellent accuracy for OD detection and blood vessel segmentation using the AIIMS infant's fundus image dataset. Figure 6 shows the results of OD detection and blood vessel segmentation on images of infant retinas.

4.2 Vessels Segmentation and Labelling

We have used the vascular feature extraction method, discussed in Section 3.3. The proposed method solves the problem of the false loop to a large extent and reduces false branches and small segment branches. We have taken several images and calculated the number of vessels correctly detected and the total number of vessels correctly detected with respect to each model for each image. Then for each model, we found out the percentage of vessels detected correctly for each image and averaged them to get the accuracy of our models. As shown in Figure 7d, for minor analysis, we have found that at least 95% of the vessel was detected correctly in all test cases, with 5% having a problem with the false loop. For major analysis, we found that almost in all test cases, principal (or main) branches are not disconnected and have an accuracy

(a)   (b)
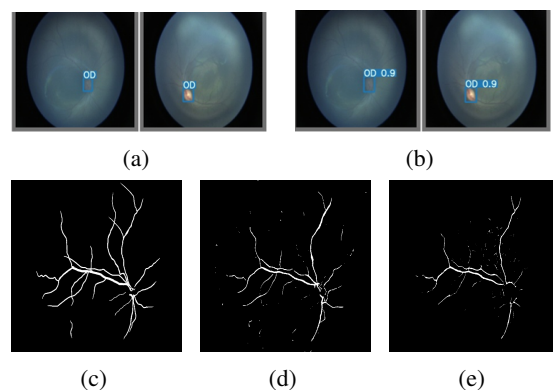

(c)   (d)   (e)

Figure 6: Example results of OD detection and blood segmentation. (a) Original OD, (b) predicted OD, (c) original blood vessels(BV) network, (d) predicted BV using Pix2Pix-GAN, and (d) predicted BV using UNet.
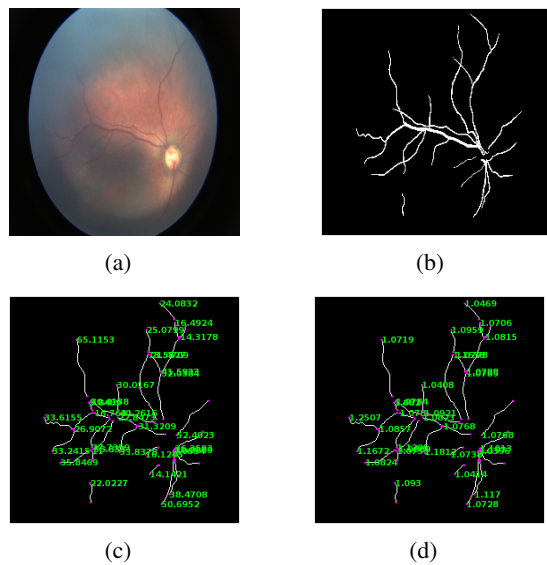
(a) (b)

(c) (d)

Figure 7: Minor analysis output. (a) Retinal image of healthy infant; (b) Blood vessels map after segmentation; (c) Length of each vessels segment (in pixels); and (d) Tortuosity value of each vessel segments.

Table 3: Plus disease classification results using tortuosity analysis of infants retinal images (Here, N/A: not applicable).

Parameters	Reference	Healthy	Pre-Plus	Plus
Score Overall	1.0894	1.126	1.1530	1.1967
Score 2nd level	1.0739	1.117	1.1530	1.1959
% of vessel infected	25%	35%	38%	56%
% of vessel severely infected	18%	20%	30%	44%
Average score (27 patient)	N/A	1.12	1.16	1.21%
Average % (27 patient)	N/A	30%	40%	55%

of around 94% overall while detecting and segmenting vessels. For ordering the vessel, the accuracy was more than 90% at 2-level classification. The accuracy falls to 60% for 3-level classification, which can be increased with some modification and changing the threshold for each specific case. Also, only a few images of the locally available datasets have three or more levels.

4.3 Plus Disease Classification

After training on a dataset of infant retinal images (Table 2), we identified a tortuosity threshold (T_H) of 1.15 for labelling a blood vessel segment as healthy or infected. Also, using this T_H (for infected vessels), we found a percentage threshold of 35% for pre-plus and 50% for Plus. In addition, we measured the cumulative range of tortuosity and found it to be between 1.13 and 1.19 for both the pre-Plus and Plus classes.
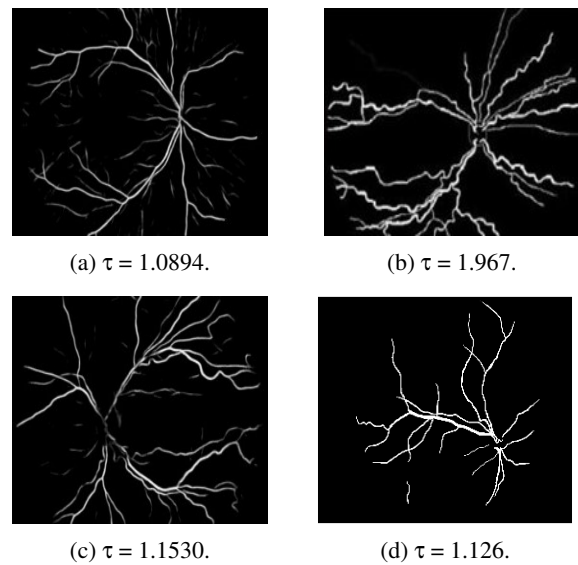

(a) $\tau = 1.0894$. (b) $\tau = 1.967$.

(c) $\tau = 1.1530$. (d) $\tau = 1.126$.

Figure 8: Plus disease classification results: (from left to right). (a) Healthy reference image use to find tortuosity threshold; (b) Plus disease; (c) Pre-Plus; and (d) Healthy.

Refer to Table 3 for results. The healthy image (from infant retinal image datasets) above has a tortuosity of 1.126 overall, and 1.1178 at the 2nd level, and the percentage of vessels infected is 35% with 20% vessels severely infected. The pre-Plus image shown above in Figure 8 has a tortuosity of 1.1530, and the percentage of vessels infected is 38%, with 30% severely infected. In contrast, the Plus image has a tortuosity of 1.1959 in the 2nd level and 1.1967 overall, with 56% of vessels infected and 44% severely infected. In comparison with the healthy reference image, it has a tortuosity of 1.0739 in the 2nd level, and 1.0894 overall, and the percentage of vessels infected is 25%, with 18% vessels severely infected. Severely infected vessels have tortuosity above 1.2, due to vessels curvature (shown in Figure 8).

5 CONCLUSION

This study presents a proof of concept (POC) for a newly proposed DL-assisted retinal disease screening system. It investigated, developed, and implemented a new classification system based on the tortuosity of retinal blood vessels to diagnose ROP-Plus disease. The proposed method allows data-driven and rule-based systems to coexist on a single platform. Consequently, it can function effectively even without a sufficient number of datasets. In addition, in this method, the doctor can view the classification results and the visualization of the detected vessels, including their segments, length, and tortuosity, to visually compre-

hend and confirm the system's decision.

In the current study, blood vessel segments that form a loop or overlap were not considered when calculating the curvature index of the vessels. In addition, the present method is trained and evaluated with a small number of retinal image datasets for three levels of ROP-Plus disease classification. Therefore, in the future, we may enhance the proposed techniques to address overlapping problems with more retinal image datasets and additional disease classification levels.

REFERENCES

Chiang, M. F., Quinn, G. E., Fielder, A. R., Ostmo, S. R., Chan, R. P., Berrocal, A., Binenbaum, G., Blair, M., Campbell, J. P., Capone Jr, A., et al. (2021). International classification of retinopathy of prematurity. *Ophthalmology*, 128(10):e51–e68.

Doi, K. (2007). Computer-aided diagnosis in medical imaging: historical review, current status and future potential. *Computerized medical imaging and graphics*, 31(4-5):198–211.

Grisan, E., Foracchia, M., and Ruggeri, A. (2008). A novel method for the automatic grading of retinal vessel tortuosity. *IEEE transactions on medical imaging*, 27(3):310–319.

Hart, W. E., Goldbaum, M., Cote, B., Kube, P., and Nelson, M. R. (1997). Automated measurement of retinal vascular tortuosity. In *Proceedings of the AMIA Annual Fall Symposium*, page 459. American Medical Informatics Association.

Heneghan, C., Flynn, J., O'Keefe, M., and Cahill, M. (2002). Characterization of changes in blood vessel width and tortuosity in retinopathy of prematurity using image analysis. *Medical image analysis*, 6(4):407–429.

Isola, P., Zhu, J.-Y., Zhou, T., and Efros, A. A. (2018). Image-to-image translation with conditional adversarial networks.

Jocher, G., Stoken, A., Borovec, J., NanoCode012, Chaurasia, A., TaoXie, Changyu, L., V, A., Laughing, tkianai, yxNONG, Hogan, A., lorenzomammana, AlexWang1900, Hajek, J., Diaconu, L., Marc, Kwon, Y., oleg, wanghaoyang0106, Defretin, Y., Lohia, A., ml5ah, Milanko, B., Fineran, B., Khromov, D., Yiwei, D., Doug, Durgesh, and Ingham, F. (2021). ultralytics/yolov5: v5.0 - YOLOv5-P6 1280 models, AWS, Supervise.ly and YouTube integrations.

Kumar, V., Patel, H., Azad, S., Paul, K., Surve, A., and Chawla, R. (2022). Dl-assisted rop screening technique. In Gehin, C., Wacogne, B., Douplik, A., Lorenz, R., Bracken, B., Pesquita, C., Fred, A., and Gamboa, H., editors, *Biomedical Engineering Systems and Technologies*, pages 236–258, Cham. Springer International Publishing.

Kumar, V., Patel, H., Paul, K., Surve, A., Azad, S., and Chawla, R. (2021). Deep learning assisted retinopathy

of prematurity screening technique. In *HEALTHINF*, pages 234–243.

Kumar., V., Patel., H., Paul., K., Surve., A., Azad., S., and Chawla., R. (2022). Improved blood vessels segmentation of retinal image of infants. In *Proceedings of the 15th International Joint Conference on Biomedical Engineering Systems and Technologies - HEALTHINF,*, pages 142–153. INSTICC, SciTePress.

MathWorks (1994-2023). Morphological operations on binary images - matlab bwmorph. https://www.mathworks.com/help/images/ref/bwmorph.html. (Accessed on 01/07/2023).

Oloumi, F., Rangayyan, R. M., and Ells, A. L. (2016). Computer-aided diagnosis of retinopathy in retinal fundus images of preterm infants via quantification of vascular tortuosity. *Journal of Medical Imaging*, 3(4):044505.

Organization, W. H. et al. (2019). World report on vision. Technical report, Geneva: World Health Organization.

Razzak, M. I., Naz, S., and Zaib, A. (2018). Deep learning for medical image processing: Overview, challenges and the future. *Classification in BioApps*, pages 323–350.

Reid, J. E. and Eaton, E. (2019). Artificial intelligence for pediatric ophthalmology. *Current opinion in ophthalmology*, 30(5):337–346.

Ronneberger, O., Fischer, P., and Brox, T. (2015). U-net: Convolutional networks for biomedical image segmentation.

Scruggs, B. A., Chan, R. P., Kalpathy-Cramer, J., Chiang, M. F., and Campbell, J. P. (2020). Artificial intelligence in retinopathy of prematurity diagnosis. *Translational Vision Science & Technology*, 9(2):5–5.

Sukkaew, L., Uyyanonvara, B., Makhanov, S. S., Barman, S., and Pangputhipong, P. (2008). Automatic tortuosity-based retinopathy of prematurity screening system. *IEICE transactions on information and systems*, 91(12):2868–2874.

Tian, P., Guo, Y., Kalpathy-Cramer, J., Ostmo, S., Campbell, J. P., Chiang, M. F., Dy, J., Erdogmus, D., and Ioannidis, S. (2019). A severity score for retinopathy of prematurity. In *Proceedings of the 25th ACM SIGKDD International Conference on Knowledge Discovery & Data Mining*, KDD '19, page 1809–1819, New York, NY, USA. Association for Computing Machinery.

Ting, D. S. W., Pasquale, L. R., Peng, L., Campbell, J. P., Lee, A. Y., Raman, R., Tan, G. S. W., Schmetterer, L., Keane, P. A., and Wong, T. Y. (2019). Artificial intelligence and deep learning in ophthalmology. *British Journal of Ophthalmology*, 103(2):167–175.

Wang, G., Li, M., Yun, Z., Duan, Z., Ma, K., Luo, Z., Xiao, P., and Yuan, J. (2021). A novel multiple subdivision-based algorithm for quantitative assessment of retinal vascular tortuosity. *Experimental Biology and Medicine*, 246(20):2222–2229.